Sustainable Engineering Materials
ISSN: 3105-1960 (Print); ISSN: 3105-1979 (Online)
http://www.sustain-dpl.com/picnews.asp?id=177
DOI: 10.54113/j.suem.2025.000004

ORIGINAL ARTICLE

Design, manufacture, and mechanical performance analysis of LVS structural plywood

Shuheng Yang[a], Zhaoyu Shen[a], Yingchao Li[b], Mahmud Ashraf[c], Zheng Wang[a*]

[a]College of Materials Science and Engineering, Nanjing Forestry University, Nanjing, Jiangsu, 210037, China
[b]Jiangsu Yindelong Wood Industry Limited Company，Lianyungang, Jiangsu,222506, China
[c]Deakin University, Geelong Waurn Ponds, VIC 3216, Australia
[*]Corresponding Author: Zheng Wang. Email: wangzheng63258@163.com

Abstract: This paper focused on Laminated Veneer Sandwich (LVS) structural plywood, systematically expounding its structural design and key production processes, and comparatively analyzing the mechanical properties such as elastic modulus of LVS and Laminated Veneer Lumber (LVL) through dynamic and static testing methods. LVS uses *populus deltoides* LVL as the core layer and Medium-Density Fiberboard (MDF) as the surface layer, adopts a "transverse-longitudinal-transverse" cross-grain composite structure, and is made through processes such as gluing, blanking, and cold pressing, effectively integrating the mechanical strength of LVL and the surface performance of MDF.Dynamic test results show that the ratio of longitudinal to transverse elastic modulus of LVS is only 13% of that of LVL, indicating that LVS is closer to an isotropic material and significantly superior to LVL in the balance of longitudinal and transverse mechanical properties. Static four-point bending tests further confirm that LVS not only has higher deformation resistance, but also has better surface flatness and coating compatibility, fully meeting the requirements of GB/T 17657—2013 and GB/T 11718—2009 standards.The research shows that LVS achieves efficient utilization of fast-growing *populus deltoides* by optimizing structural design and process parameters, boasts broad application prospects in construction, furniture, decoration, and other fields, and is of great significance for promoting the upgrading of China's wood processing industry and realizing a win-win situation of economic and social benefits.

Keywords: LVS; LVL, Structural design and process, Dynamic testing, Modulus of elasticity

1 Introduction

In the 1970s, the United States pioneered the development of Laminated Veneer Sandwich (LVS), a novel composite material in the wood processing industry. LVS subsequently experienced rapid growth and widespread adoption in developed countries such as Japan and North America. In China, Xuzhou Nanlin Wood Industry Co., Ltd. established and operationalized an annual production line of 20,000 m^3 LVS in 2005. By 2017, Lianyungang Gongliang Wood Industry Co., Ltd. achieved an annual output of 2,500 m^3 of structurally enhanced *Populus deltoides* LVS products, becoming the sole domestic enterprise exporting LVS to Japan [1-3].

Received: 15 April 2025; Received in revised form: 22 July 2025; Accepted: 25 July 2025

LVS employs *Populus deltoides* multi-layer plywood or LVL (Laminated Veneer Lumber) as the core material and medium-thick or thin MDF (Medium Density Fiberboard) as the surface material. These layers are bonded with adhesive, assembled, and cold-pressed, effectively addressing traditional shortcomings of *Populus deltoides* plywood, such as warping, deformation, cracking, and poor color retention [4-6].

Combining the strengths of LVL and MDF, LVS exhibits near-isotropic properties, superior physical-mechanical performance, and exceptional deformation resistance. The composite structure also resolves common plywood limitations, including poor moldability and inadequate decorative appeal. Consequently, LVS is extensively utilized in solid wood composite doors (frames and panels), sliding doors, window frames, cabinets, partitions, and backing boards.

This study optimizes the structural design and key production processes of *Populus deltoides* LVS structural plywood and implements non-destructive mechanical testing on the final product [7-9].

The results demonstrate LVS's high dimensional stability, robust deformation resistance, smooth surface finish, and excellent decorative and coating compatibility. These properties enable LVS to meet diverse demands across industries such as construction, furniture, interior design, transportation, and military applications, underscoring its significant practical value and economic potential.

2 LVS Structure Design and Production Process

2.1 Structural design

Developed in this study, the novel *Populus deltoides* LVS structural plywood was manufactured in accordance with standards GB/T 17657–2013 (Test Methods for Physical and Chemical Properties of Wood-based Panels and Surface-decorated Wood-based Panels) and GB/T 11718–2009 (Medium Density Fiberboard), with panel dimensions of 2,440 × 1,220 × 24 mm (length × width × thickness).

The LVS panel features a three-layer composite structure: a laminated veneer lumber (LVL) core sandwiched between upper and lower medium-density fiberboard (MDF) surface layers. To enhance deformation resistance, the LVL core adopts a cross-grain orientation with a transverse-longitudinal-transverse (T-L-T) configuration, as supported by **Fig. 1**.

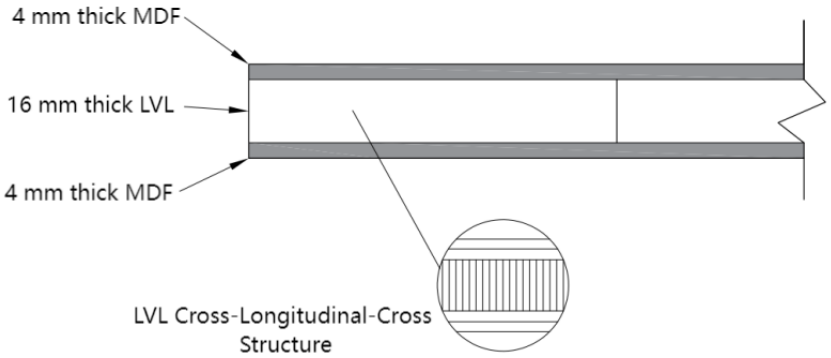

Fig. 1. Structural design drawing of LVS plate

2.2 Material

The LVS core layer incorporates fast-growing *Populus deltoides* LVL panels (8%–12% moisture content), supplied by Lianyungang Gongliang Wood Industry Co., Ltd. These LVL panels were manufactured by rotary-cutting logs into 2 mm-thick veneers, followed by multi-layer longitudinal lamination, pre-pressing, hot-pressing, curing, and sawing. Standard panel thicknesses range from 16–75 mm. To enhance deformation resistance, the *Populus deltoides* LVL core was structurally optimized through equal-width and equal-thickness longitudinal cutting, followed by transverse-longitudinal-transverse (T-L-T) triple-layer cross-grain bonding to mitigate warping.

The upper and lower surface layers employ JIS-compliant moisture-resistant medium-density fiberboard (MDF; Model: DSK-M0-2105, DAIKEN Corporation, Malaysia) with sanded surfaces and thickness tolerance controlled within ± 0.15 mm.

Adhesives: Urea-formaldehyde (UF) resin-flour hybrid adhesive (flour-to-resin ratio 3:7),

supplied by Henan Shenghongfeng Chemical Co., Ltd. Edge-bonding adhesive (Model 301), with a solid content of (40±2)% and viscosity of 450-500 mPa·s, produced by Liuyang Tianhe Adhesive Factory.

2.3 Equipment

Primary equipment for LVS panel fabrication included drying systems, adhesive applicators, pre-pressing units, hot presses, and high-frequency edge-bonding machines, as detailed in Table 1.

Tab 1. Main production equipment of LVS

Device	Manufacturer/Model	Purpose	Main parameters
Dryer	Shandong Linyi Pengyuanlong Machinery Co., Ltd.	Dry the veneer, reducing its moisture content.	Motor power is 4 kW; the heating temperature is between 120~150 ℃; the drying time in winter is 1 hour, and in summer it is 25~30 minutes; the moisture content of the board is between 7%~10%.
Glue Applicator	Qingdao Jianlong Machinery Co., Ltd.	Single board glue application	Hybrid adhesive composed of flour and urea-formaldehyde resin ; Glue spread: 250 – 300 g/m^2 ; Applied via roller coating ; Parallel-to-grain assembly
Pre-press machine	Shandong Linyi Pengyuanlong Machinery Co., Ltd.	Cold pressing	Standard pressure is 0.9~1.2 MPa; gauge pressure is 0.7~2.2 MPa; cold press time is (35±10) minutes; motor power is 4 kW.
Hot press machine	Shandong Linyi Pengyuanlong Machinery Co., Ltd.	Hot pressing	Standard pressure is 0.8~1.0 MPa; gauge pressure is 0.7~2.0 MPa; steel plate temperature is 100~125 ℃; hot pressing time is product thickness × 1.3; motor power is 4 kW.
Belt Sander	Qingdao Freedom Machinery Manufacturing Co., Ltd., (BSG2613)	Sanding to a fixed thickness	Working pressure is 0.55 MPa; feed rate is 4~30 m/min; processing width is 40~1,300 mm; processing thickness is 3~120 mm; total motor power is 120.5 kW.
High-frequency panel bonding machine	Shijiazhuang Qinchuan Machinery Co., Ltd., (SP20-SA)	LVL Cross-Longitudinal-Cross Edge Splicing Processing	The processing range is 1,220~2,400 mm; the frequency is 6.73 MHz; the output power is 20 kW; the system pressure is 16 MPa, and the actual pressure is 6 MPa.

2.4 Manufacturing process

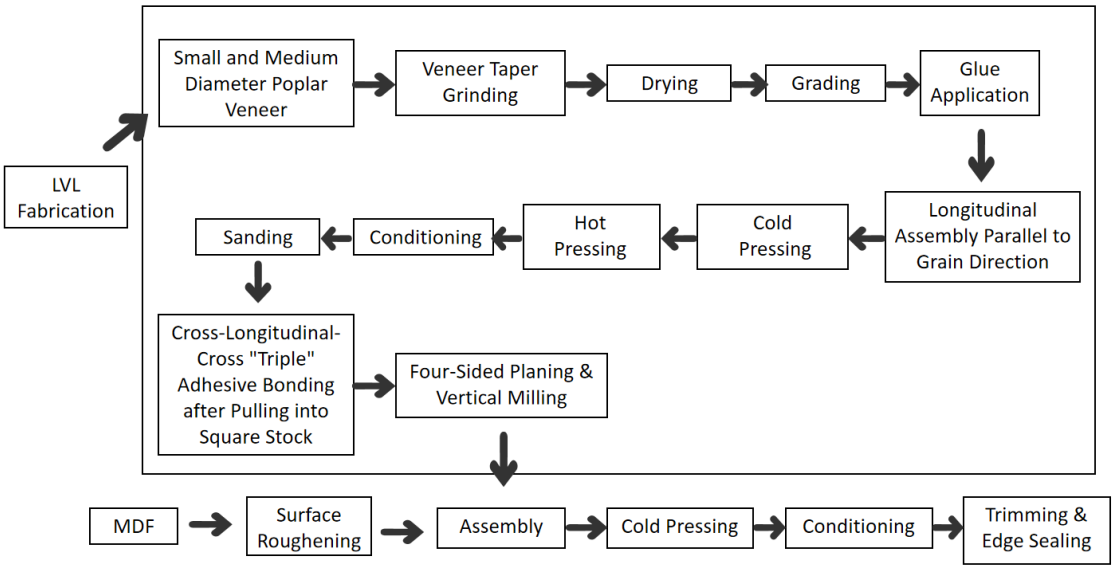

Fig.2 Production flow chart of LVS plate

The novel manufacturing process for *Populus deltoides* LVS structural plywood developed in this study is schematically illustrated in Fig. 2. Sections 2.4.1 to 2.4.6 present the specific production processes and technological parameters of LVS.

2.4.1 LVL Material Preparation:

Raw logs are rotary-cut into 2 mm-thick veneers, followed by bevel grinding, drying, grading, glue application, longitudinal grain-oriented layup, cold pressing (pre-pressing), and hot pressing to produce LVL.

2.4.2 Cutting & Dimensioning:

After 7-10 days of curing, LVL panels are sawn and sanded to reach the target thickness. Quality grading is conducted after sanding, and panels that fail to meet the thickness specifications are reprocessed.

2.4.3 Adhesive Bonding & Layup:

Calibrated LVL panels are subjected to strip cutting to meet product dimensions. Double-sided roller coating (with a glue spread rate of 250 – 300 g/m^2) is manually applied along the edge-bonding direction by operators. After a 30-minute open assembly period, the strips are assembled into a "transverse-longitudinal-transverse" cross-grain configuration using a high-frequency edge-bonding machine.

2.4.4 Sanding, Profiling & Trimming:

Edge-bonded LVL panels are sanded to calibrate their thickness, after which they are processed through a four-sided planer to achieve surface smoothing and profile shaping.

2.4.5 MDF Surface Lamination:

Single-sided roller coating is applied on MDF using an MT6213 glue spreader (glue spread rate: 210 – 230 g/m^2).The MDF was assembled with LVL to form LVS panels.

2.4.6 Cold Pressing, Curing & Finishing:

LVS panels are pre-pressed to ensure adhesive penetration, uniform distribution, and excess glue removal, which enhances bonding strength. The panels are then stacked to a 1.1 m height and cold-pressed at 0.9 MPa for 60 minutes. After curing for 72 hours, the panels undergo trimming and edge sealing. **Fig. 4** illustrates the cold-pressing process of LVS.

Fig.3. LVS-laminated facing assembly

Fig.4. Cold pressing of LVS plate

The quality of LVL veneers directly impacts the final product. Key factors affecting veneer quality include: manufacturing-induced defects, which include lathe check depth (backside fissures), surface roughness, thickness deviation, and moisture content variability; inherent wood variability, encompassing knots, cracks, density fluctuations, spiral grain, species differences, and growth ring effects.

Production observations reveal a strong correlation between LVL veneer thickness and lathe check severity—thicker veneers exhibit deeper backside fissures [10-13]. Experimental data demonstrate that replacing rotary cutting with high-precision sawing eliminates lathe checks while minimizing thickness deviations.

To address warping during rapid veneer drying, this study implements steam-jet rapid drying technology, which reduces energy consumption while maintaining veneer flatness [14-16].

The following presents a dynamic testing and comparative analysis of the elastic modulus between LVS Plywood and LVL.

3 Dynamic Testing and Analysis of LVS and LVL Modulus of Elasticity

In China, plywood manufacturers primarily assess panel quality through conventional static bending tests (measuring modulus of rupture [MOR] and modulus of elasticity [MOE]) and visual inspection. The present study employs the free-plate transient excitation method for dynamic MOE evaluation of LVL and LVS products, offering rapid, simple, highly repeatable, and precise non-destructive assessment.

3.1 Testing Equipment

The testing equipment employed in this study includes the following components: 1 set of CRAS Vibration Signal Acquisition and Analysis System, which comprises an AZ-308 data acquisition unit, an AZ-802 signal conditioning unit, and SSCars software (supplied by Nanjing Anzheng Software Engineering Co., Ltd.); 1 unit of CA-YD-125 accelerometer, with key parameters of 15.9 pC/(m • s^2) in sensitivity and 0 – 20,000 Hz in frequency response range (manufactured by Yangzhou Jufeng Technology Co., Ltd.); 1 set of custom-made free-hanging support frame; and 1 unit of rubber mallet.

3.2 Specimen Preparation

Specimens were prepared from *Populus deltoides* LVL and LVS panels manufactured using the aforementioned methods. Dimensions and quantities are summarized in **Table 2**:

LVL specimens: 780 mm × 128 mm × 16 mm ($L \times W \times T$), 12 units (6 longitudinal, 6 transverse); density 589 kg/m³; moisture content 10%. LVS specimens: 860 mm × 144 mm × 24 mm ($L \times W \times T$), 12 units (6 longitudinal, 6 transverse); density 650 kg/m³; moisture content 10%.

Tab.2 Specification and quantity of test pieces

Specimen	Specification size (mm)	Quantity (Block)
LVL（Lateral）	780×128×16	6
LVL（Vertical）	780×128×16	6
LVS（Lateral）	860×144×24	6
LVS（Vertical）	860×144×24	6

3.2 Testing principles and main steps

The longitudinal and transverse elastic moduli of LVL and LVS specimens were dynamically tested using the free-plate transient excitation method. This method, based on beam theory, correlates the first-order bending frequency of a freely supported plate with its elastic modulus. The relationship between the first-order bending frequency (f_1) and the elastic modulus (E) is expressed as **Equation (1)** [17]:

$$E = 0.9462\rho\frac{l^4 f_1^2}{h^2} \tag{1}$$

In the equation: E is the elastic modulus of the specimen (Pa); ρ is the Density (kg/m³); f_1 is the First-order bending frequency of the specimen (Hz); L is the Length of the specimen (m); h is the Thickness of the specimen (m).

By substituting the specimen’s dimensional parameters and first-order bending frequency values into the equation, the dynamic elastic modulus of the specimen can be calculated. The following steps were adopted in the dynamic testing procedure.

Specimen Mounting:

The LVS specimen is suspended at 0.224L and 0.776L from one end using rubber bands to achieve a free-plate constraint configuration. Subsequently, the vibration testing system is connected, and the accelerometer is securely attached to the specimen surface, as shown in **Fig. 5.**

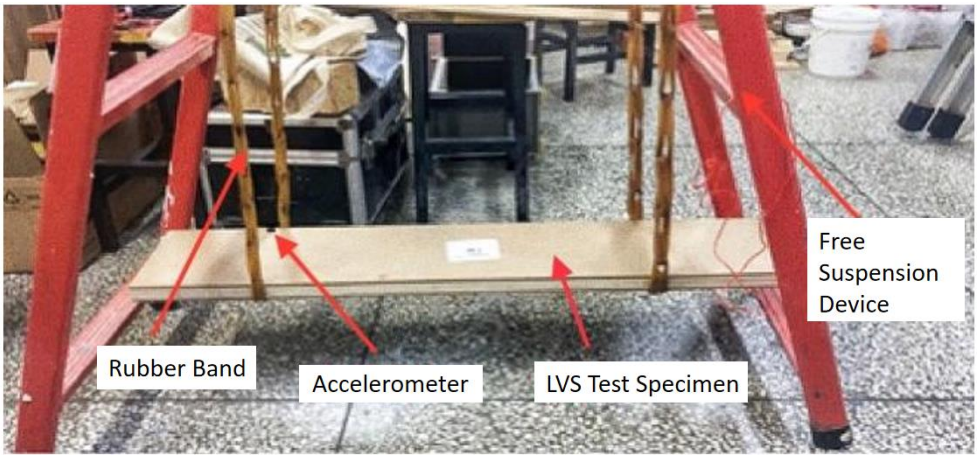

Fig.5. LVS specimen test

Signal Acquisition Setup:

The signal acquisition software is configured with an analysis frequency of 200 Hz, FFT length of 4,096, negative trigger mode, and voltage range of ±5,000 mV. Signal integrity is verified by ensuring appropriate acceleration response amplitudes.

Excitation & Data Collection:

The specimen is struck transversely with a rubber mallet to induce free vibration. Mechanical vibrations are converted into electrical signals by the accelerometer, which are then amplified, filtered, and processed via Fourier transformation to generate a frequency spectrum of transverse vibrations.

Frequency Extraction & Calculation:

The first-order bending frequency (f_1) is identified from the spectrum and substituted into the formula to calculate the elastic modulus (E).

3.4 Results and Analysis

Tab.3 Elastic modulus test of LVL specimen

Direction	Specimen Number	Moisture content (%)	Density ($kg \cdot m^{-3}$)	First-order bending frequency (Hz)	Elastic modulus (MPa)	Average Elasticity Modulus (MPa)	Coefficient of Variation (%)
Vertical	A-1	9.5	593	123.4	12 103	12 397	2.09
	A-2	8.5	591	123.4	12 255		
	A-3	8.5	585	125.9	12 614		
	A-4	9.0	582	124.7	12 181		
	A-5	9.0	590	126.9	12 848		
	A-6	9.0	591	124.7	12 383		
Lateral	B-1	9.5	617	31.88	862	864	1.72
	B-2	8.5	604	32.5	873		
	B-3	9.0	610	32.19	861		
	B-4	9.0	606	31.88	839		
	B-5	9.5	606	32.19	860		
	B-6	9.0	626	32.19	888		

Table 3 shows the test results of LVL, and Table 4 shows those of LVS, respectively. The longitudinal elastic modulus of LVL is 12397 MPa, and the transverse elastic modulus is 864 MPa, with a significant difference between the two values. The average longitudinal elastic modulus of LVS is

6898 MPa, the transverse elastic modulus is 3586 MPa, and the average density is 650 kg/m³ , which meets the quality requirements specified in GB/T 17657-2013 Test Methods for Physico-chemical Properties of Wood-based Panels and Decorated Wood-based Panels and GB/T 11718-2009 Medium Density Fiberboard (average longitudinal elastic modulus ⩾ 4000 MPa, density ⩾ 600 kg/m³).

Tab.4 Elastic modulus test of LVS specimen

Direction	Specimen Number	Moisture content (%)	Density ($kg \cdot m^{-3}$)	First-order bending frequency (Hz)	Elastic modulus (MPa)	Average Elasticity Modulus(MPa)	Coefficient of Variation (%)
Vertical	A-1	9.5	649	107.2	6 736	6 898	4.84
	A-2	10.0	647	109.7	6 997		
	A-3	9.5	649	108.4	6 845		
	A-4	10.0	660	110.3	7 224		
	A-5	10.0	658	110.9	7 292		
	A-6	9.0	634	105.3	6 292		
Lateral	B-1	10.5	645	78.44	3 589	3 586	0.71
	B-2	9.5	656	77.50	3 536		
	B-3	9.5	652	78.13	3 587		
	B-4	10.0	655	78.13	3 617		
	B-5	9.5	644	78.75	3 577		
	B-6	9.0	650	78.44	3 606		

Tab.5 Comparison of physical and mechanical properties between LVS plywood and LVL

Project	LVL	LVS
Plate thickness mm	16	24
Density $kg \cdot m^{-3}$	589	650
Longitudinal Elastic Modulus MPa	12 397	6 898
Transverse Elastic Modulus MPa	864	3 586
Lateral to longitudinal modulus ratio	14.3	1.9

As indicated in **Table 5**, the longitudinal-to-transverse elastic modulus ratio of LVL is 14.3, significantly higher than that of LVS (1.9). This demonstrates that LVS is closer to an isotropic material compared to LVL, with more balanced mechanical properties in both longitudinal and transverse directions, resulting in broader applicability. Evidently, LVS leverages the combined advantages of LVL and MDF, offering superior performance in deformation resistance, surface decoration, and coating compatibility, underscoring its significant practical advantages.

4 Static Testing and Analysis of Elastic Modulus for LVS and LVL

This experiment also employed static testing methods to determine the elastic modulus values of LVS and LVL materials. The static tests utilized the four-point bending method, which is categorized into symmetric four-point bending tests and asymmetric four-point bending tests.

4.1 Materials

The LVS and LVL materials used in this study are defined with the following coordinate system: X-direction: Longitudinal (L) direction in-plane; Y-direction: Transverse (T) direction in-plane. Z-direction: Out-of-plane thickness (R) direction.

The specimen orientation is represented by a three-axis notation system, where: The first letter denotes the longitudinal direction of the specimen. The second letter denotes the transverse direction of the specimen. The omitted third letter (implicit) represents the thickness direction.

For example: LVL-X-1 means Specimen 1 of LVL with the X-direction (longitudinal) as the primary axis; LVS-Y-2 means Specimen 2 of LVS with the Y-direction (transverse) as the primary axis.

The dimensions and physical properties of the specimens are as follows:

LVS specimens: 380 mm × 24 mm × 24 mm, with an average air-dry density of 650 kg/m ³and 530 kg/m ³ and a moisture content of 9–11%.

LVL specimens: 380 mm × 16 mm × 16 mm, with an average air-dry density of 797 kg/m ^{3}and a moisture content of 9–11%.

The detailed specifications and quantities of the specimens are listed in **Table 6**.

Tab.6 Specification and quantity table of test pieces

Material	Specimen Designation	Specification (mm^3)	Quantity / Block
LVS	X-direction beam	380 ×24 ×24	6
	Y-direction beam	380 ×24 ×24	6
LVL	X-direction beam	380 ×16 ×16	6
	Y-direction beam	380 ×16 ×16	6

4.2 Testing Instruments

The testing equipment utilized in this study consists of the following components: 1 set of CRAS Vibration and Dynamic Signal Acquisition and Analysis System (Nanjing Anzheng Software Engineering Co., Ltd.), which includes an AZ-408 data acquisition unit, an AZ-802 signal conditioning unit, CRAS AdCras data acquisition and processing software, and CRAS SsCras signal and system analysis software; 1 set of KD6005 strain amplifier (Yangzhou Kedong Electronics Co., Ltd.) equipped with multiple bridge boxes and connecting cables; 1 unit of CMT5105 microcomputer-controlled electronic universal testing machine (Shenzhen Sansi Zongheng Technology Co., Ltd.) with an accuracy class of 0.5 and a maximum test force of 100 kN; BX120-5AA resistance strain gauges (Zhejiang Huangyan Testing Instrument Factory) with grid dimensions of 5 mm × 3 mm, a resistance of 119.7 ± 0.1 Ω, and a sensitivity coefficient of 2.08 ± 1%; and 1 set of four-point bending test fixture, which includes weights and cables.

4.2 Four-Point Bending Tests for LVL and LVS Specimens

Static four-point bending tests were conducted on specimens in both the X- and Y-directions. This study first employed Yoshihara’s asymmetric four-point bending method [18-24] to determine the shear modulus of LVL and LVS specimens. Subsequently, the testing setup and specimen placement were further adjusted to achieve symmetric four-point bending loading, thereby enabling the measurement of the elastic modulus and Poisson’s ratio for LVL and LVS specimens.

4.3 Testing Methods and Principles

In the four-point bending test, the symmetric four-point bending method is used to measure the elastic modulus and Poisson’s ratio of specimens, while the asymmetric four-point bending method is employed to determine the shear modulus. For the same specimen, the static elastic modulus and static shear modulus can be measured by modifying the support configuration and span of the loading beams, as well as adjusting the loading surface orientation.

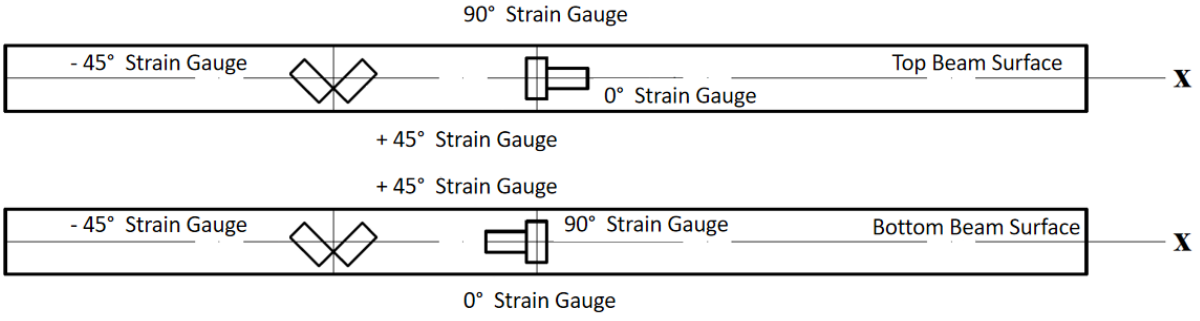

Fig.6. Schematic diagram of strain gauge pasting

In the four-point bending test, the symmetric four-point bending method is used to measure the elastic modulus and Poisson’s ratio of specimens, while the asymmetric four-point bending method is employed to determine the shear modulus. For the same specimen, the static elastic

modulus and static shear modulus can be measured by modifying the support configuration, adjusting the span of the loading beams, and reorienting the loading surface. The testing principle involves bonding 0 °and 90 °strain gauges (termed 0-90 °gauges) and +45 °and -45 °strain gauges (termed ±45 ° gauges) to the mid-span of two symmetrical planes of the beam specimen (as shown in **Fig.6**). In the symmetric four-point bending setup, the support span is defined as L, with strain gauge planes parallel to the ground. A loading beam of length L/3 is positioned at the mid-span to establish symmetric loading (as shown in **Fig.7**). Weights are then applied to the loading beam, creating a pure bending region in the central L/3 segment, where the bottom surface undergoes tension and the top surface experiences compression. Electrical signals from the strain gauges are amplified by the strain amplifier, processed through the dynamic signal acquisition and analysis system for signal conditioning and A/D conversion, and recorded as time-domain signals. The mean value of these signals represents the strain measurement. Loads are applied incrementally, and the mean strain differences from the 0 ° and 90 ° gauge readings are calculated. The elastic modulus (E) can be calculated using **Equation (2)**, and Poisson's ratio (μ) can be calculated using **Equation (3)**.

$$E = \Delta\rho \frac{10^6 l}{bh^2 \bar{\varepsilon}_{0^\circ}} \tag{2}$$

Where: l is the specimen length (unit: m), b is the specimen width (unit: m), h is the specimen thickness (unit: m), $\bar{\varepsilon}_{0^\circ}$ is the mean strain difference of the 0 ° gauge in symmetric four-point bending (unit: με), ΔP is the incremental load applied during each step of weight addition (unit: N).

$$\mu = \bar{\varepsilon}_{0^\circ} / \bar{\varepsilon}_{90^\circ} \tag{3}$$

Where: $\bar{\varepsilon}_0$ is the mean strain difference of the 0 °gauge in symmetric four-point bending (unit: με), $\bar{\varepsilon}_{90^\circ}$ is the mean strain difference of the 90 °gauge in symmetric four-point bending (unit: με).

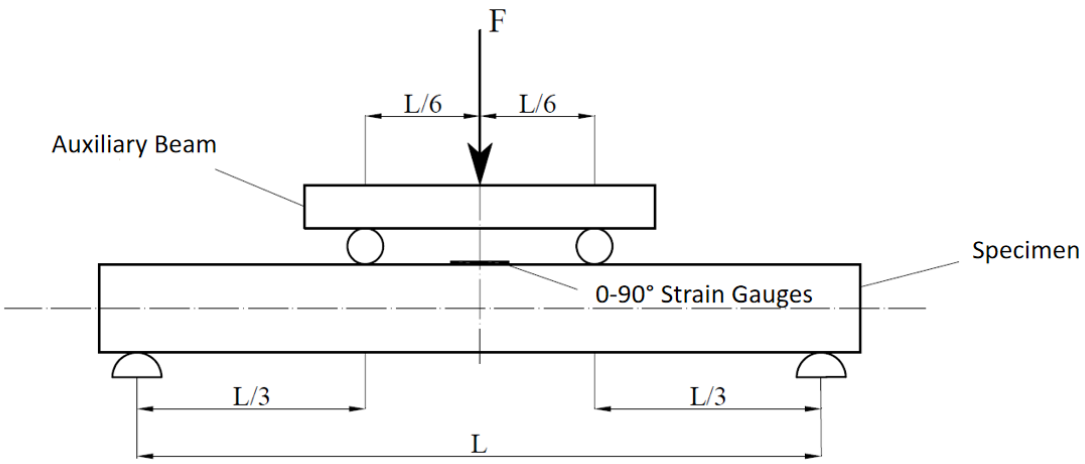

Fig.7. Schematic diagram of symmetrical four-point bending test

To establish the asymmetric four-point bending system, the support span is adjusted to 2/3L, and the beam specimen is rotated 90 ° about its longitudinal axis and repositioned on the supports. In this configuration, the width and height of the specimen under symmetric four-point bending are interchanged to represent the height and width in the asymmetric state, respectively. The plane containing the strain gauges is now perpendicular to the ground. A loading beam of length 2/3L is placed at the 2/3L end on the opposite side of the specimen, completing the asymmetric four-point bending setup (as shown in **Fig 8**). Weights are applied to the loading beam, inducing shear stress on the surface where the strain gauges are bonded. Based on the stress-strain relationship, the strain increments obtained from the ±45 ° strain gauge readings are substituted into the **Equation (4)** to calculate the shear modulus (G) of the specimen in the plane containing the ±45 °gauges:

$$G = \frac{3\times10^{6}\Delta p}{8hb\Delta\varepsilon} \tag{4}$$

Where: b is the specimen width (unit: m); h is the specimen thickness (unit: m); $\Delta\varepsilon$ is the strain increment measured by the full-bridge circuit in asymmetric four-point bending (unit: με); ΔP is the incremental load applied during each step of weight addition (unit:N).

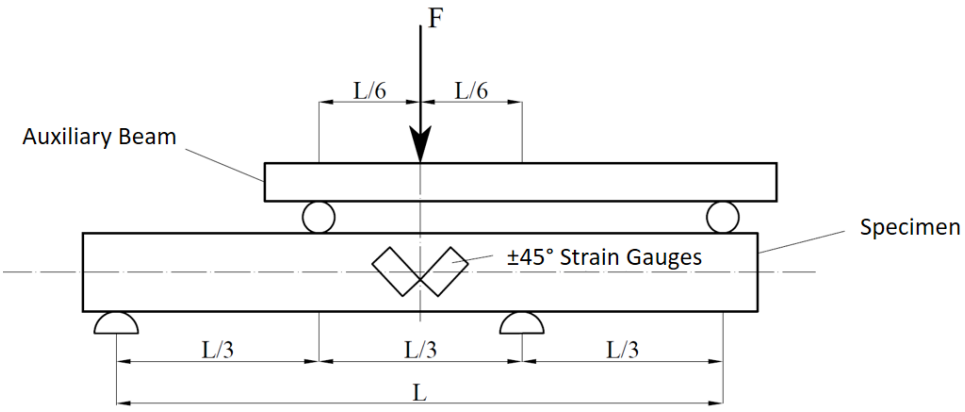

Fig.8. Schematic diagram of asymmetrical four-point bending test

4.4 Testing Procedure

4.4.1Symmetric Four-Point Bending (Example: X-direction beam, XY-plane)

First, strain gauge installation was performed by bonding 0 °and 90 °strain gauges at the mid-span of the two XY-planes on the X-direction beam. Subsequently, for instrumentation setup, the strain gauges were wired to the bridge box and strain amplifier, with the amplifier further connected to Channels 1 and 2 of the dynamic signal acquisition and analysis system—specifically, the 0 ° gauge (configured in a half-bridge circuit) to Channel 1 and the 90 ° gauge (also in a half-bridge circuit) to Channel 2—followed by system parameter configuration. In the loading and data acquisition phase, weights were applied incrementally; strain values of the 0 °and 90 °gauges were recorded once readings stabilized. The specimen was then rotated 180 °around its longitudinal axis to repeat the test. Finally, the static elastic modulus and Poisson's ratio were calculated using the strain data obtained from both XY-planes.

4.4.2Asymmetric Four-Point Bending (Example: X-direction beam, XY-plane)

First, ±45 °strain gauges were bonded onto the two XY-planes of the X-direction beam for strain gauge installation. Next, in the instrumentation setup phase, the strain gauges were wired to the bridge box and strain amplifier, with the amplifier further connected to Channel 1 of the dynamic signal acquisition system; a full-bridge circuit was configured as follows: the front +45 ° gauge to Terminals 1–2, the rear −45° gauge to Terminals 2–3, the rear +45 ° gauge to Terminals 3–4, and the front −45° gauge to Terminals 1–4, followed by setting the system parameters. Subsequently, for the loading system configuration, the support span was adjusted to 2/3L, the specimen was positioned with its test surface (XY-plane) facing forward, and a 2/3L-span auxiliary loading beam was placed at the opposite end to establish an asymmetric four-point bending system. Finally, in the loading and data acquisition step, weights were applied incrementally, strain values of the ±45 °gauges were recorded once readings stabilized, the specimen was rotated 180 °around its longitudinal axis to repeat the test, and the static shear modulus was calculated using strain data from both XY-planes.

The testing procedure for Y-direction beams follows the same steps as described for X-direction beams. All tests are conducted within the elastic deformation range of the specimens. Each specimen undergoes three repeated trials, and the results are averaged to minimize experimental errors. **Fig. 9** shows the on-site testing of the LVL-B-Y-2 specimen using the symmetric four-point bending method; **Fig. 10** shows the on-site testing of the YX plane of the LVS-B-Y-1 specimen using the asymmetric four-point bending method.

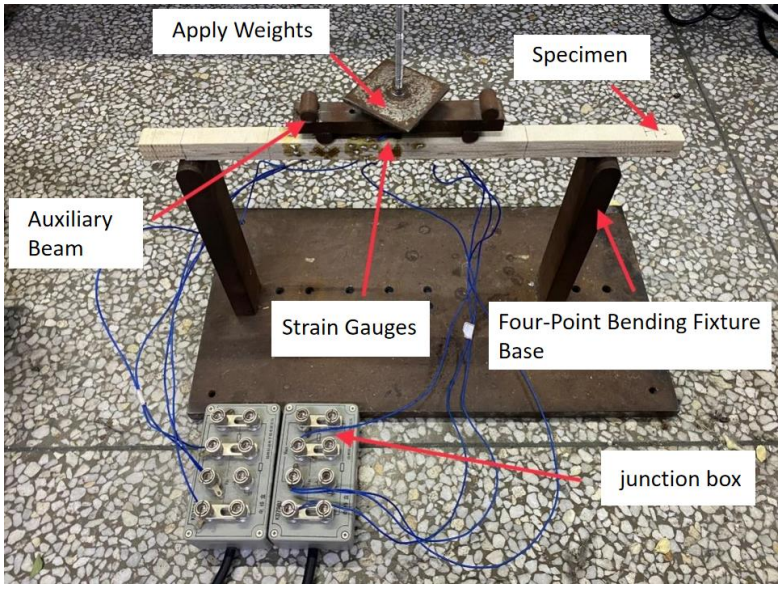

Fig.9. LVL-B-Y-2 symmetrical four-point bending test

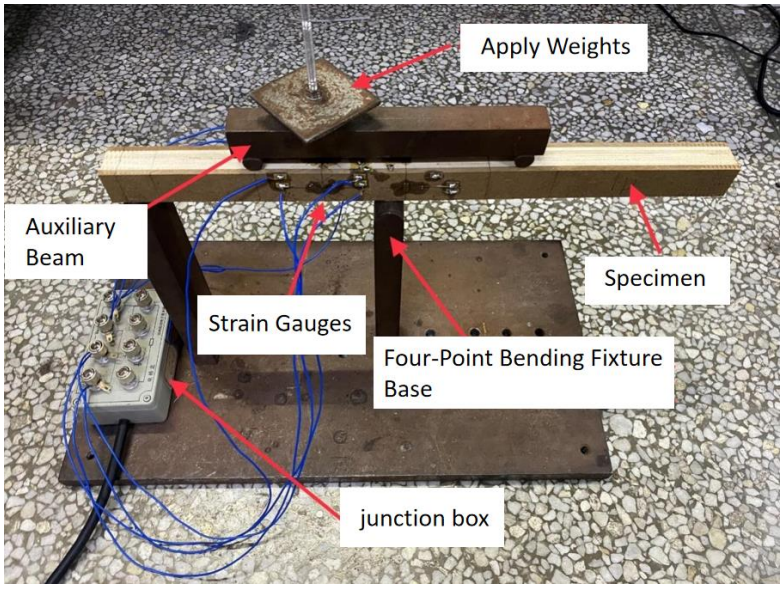

Fig10. LVS-B-Y-1asymmetrical four-point bending test

4.5 Test Results and Analysis

The static four-point bending test results for the elastic modulus, Poisson's ratio, and shear modulus of LVL beams in the X- and Y-directions are summarized in **Tables 7 to 8.**

Tab.7 Four-point bending test data sheet of LVL beam specimen in X direction

Specimen ID	Length (mm)	Width (mm)	Thickness (mm)	E_{XY} (MPa)	E_{XZ} (MPa)	μ_{XY}	μ_{XZ}	G_{XY} (MPa)	G_{XZ} (MPa)
LVL-B-X-1	380	15.6	15.6	11484	10741	0.496	0.367	969	1035
LVL-B-X-2	380	16.1	15.6	9524	10882	0.377	0.350	938	1041
LVL-B-X-3	380	15.6	15.6	11314	11353	0.448	0.392	801	1161
LVL-B-X-4	380	15.8	15.6	11876	11386	0.406	0.387	1086	1026
LVL-B-X-5	380	16.0	15.6	10254	10507	0.487	0.378	845	1099
LVL-B-X-6	380	15.7	15.6	9914	11019	0.428	0.334	811	1112
Mean				10774	10992	0.440	0.368	903	1079
Coefficient of Variation(%)				8.2	2.4	11.1	6.7	8.1	5.4

Tab.8 Four-point bending test data sheet of LVL beam specimen in Y direction

Specimen ID	Length (mm)	Width (mm)	Thickness (mm)	E_{XY} (MPa)	E_{XZ} (MPa)	μ_{XY}	μ_{XZ}	G_{XY} (MPa)	G_{XZ} (MPa)
LVL-B-Y-1	380	15.6	15.6	612	644	0.037	0.354	674	240
LVL-B-Y-2	380	16.1	15.6	474	594	0.045	0.374	801	212
LVL-B-Y-3	380	15.6	15.6	628	738	0.035	0.296	767	286
LVL-B-Y-4	380	15.8	15.6	495	601	0.032	0.281	821	209
LVL-B-Y-5	380	16.0	15.6	634	751	0.041	0.403	724	290
LVL-B-Y-6	380	15.7	15.6	584	625	0.044	0.339	696	239
Mean				571	659	0.039	0.341	747	246
Coefficient of Variation(%)				12.1	9.1	6.2	9.7	7.2	12.4

The static four-point bending test results for the elastic modulus, Poisson's ratio, and shear modulus of LVS beams in the X- and Y-directions are presented in **Tables 9 to 10.**

Tab.9 Four-point bending test data sheet of LVS beam specimen in X direction

Specimen ID	Length (mm)	Width (mm)	Thickness (mm)	E_{XY} (MPa)	E_{XZ} (MPa)	μ_{XY}	μ_{XZ}	G_{XY} (MPa)	G_{XZ} (MPa)
LVS-B-X-1	380	24.3	24.0	7323	10273	0.271	0.469	1189	807
LVS-B-X-2	380	24.2	24.0	7205	10041	0.286	0.408	1226	739
LVS-B-X-3	380	24.2	24.0	7575	9779	0.295	0.418	1219	739
LVS-B-X-4	380	23.9	24.0	6835	10129	0.272	0.428	1178	805
LVS-B-X-5	380	24.2	24.0	7306	10045	0.303	0.405	997	786
LVS-B-X-6	380	23.9	24.0	7164	9998	0.258	0.457	1309	760
Mean				7235	10055	0.281	0.431	1203	773
Coefficient of Variation(%)				3.7	1.8	3.6	5.4	8.1	4.3

Tab.10 Four-point bending test data sheet of LVS beam specimen in Y direction

Specimen ID	Length (mm)	Width (mm)	Thickness (mm)	E_{XY} (MPa)	E_{XZ} (MPa)	μ_{XY}	μ_{XZ}	G_{XY} (MPa)	G_{XZ} (MPa)
LVS-B-Y-1	380	23.3	24.0	3600	2283	0.261	0.356	819	233
LVS-B-Y-2	380	23.4	24.0	3326	2566	0.263	0.362	889	235
LVS-B-Y-3	380	23.6	24.0	3378	2504	0.254	0.360	795	251
LVS-B-Y-4	380	23.9	24.0	3561	2706	0.267	0.359	776	257
LVS-B-Y-5	380	24.0	24.0	3328	2401	0.250	0.363	881	233
LVS-B-Y-6	380	23.6	24.0	3415	2246	0.261	0.355	846	229
Mean				3435	2451	0.259	0.359	834	240
Coefficient of Variation(%)				3.5	5.0	1.5	0.7	4.8	3.4

As evident from Tables 7 to 10, the elastic modulus measured on the XY plane of LVL specimens is close to that measured on the XZ plane, while the Poisson's ratio of the XZ plane accounts for 84% of that of the XY plane. The elastic modulus and Poisson's ratio of the XY plane for the LVL-B-X-2 specimen exhibit significant discreteness. Due to the relatively small cross-sectional area of the specimens, the influence of wood grain is substantial, and the anisotropy of LVL is evident; thus, the coefficient of variation of the Poisson's ratio on the XY plane reaches 11.1%. The coefficients of variation for E_{YX} and μ_{YX} measured on the YX plane of the Y-direction beam are 12.1% and 9.1%, respectively, indicating that the mechanical properties of the X-direction beam specimens are more stable compared with those of the Y-direction beam specimens. Additionally, the magnitude relationship between the shear moduli of the XY and XZ planes in the X direction is opposite to that in the Y direction: G_{XY} in the X direction is smaller than G_{XZ}, whereas G_{YX} in the Y direction is significantly larger than G_{YZ}.

For LVS, the elastic modulus measured on the XY plane is 72% of that measured on the XZ plane, the Poisson's ratio on the XY plane is 65% of that on the XZ plane, and the shear modulus on the XY plane is 220% of that on the XZ plane. For the Y-direction beam, the elastic modulus, Poisson's ratio, and shear modulus on the YX plane are 140%, 72%, and 348% of those on the YZ plane, respectively.

The coefficients of variation for the elastic constants measured from both the X-direction and Y-direction beam specimens are less than approximately 8%, indicating that the mechanical properties of the LVS material are more stable.

5 Results and Analysis

This paper introduces the structural design and manufacturing processes of LVS plywood and conducted a comparative study on the dynamic and static elastic modulus of LVS and LVL. The research demonstrates that LVS, composed of LVL and MDF, exhibits higher stiffness and more balanced mechanical properties compared to LVL. The upper and lower MDF layers significantly enhance the elastic modulus and shear modulus of LVS, rendering it closer to an isotropic material with improved mechanical stability. The production of LVS achieves "efficient utilization of low-grade and small-sized wood" and meets application demands in construction, furniture, decoration, transportation, and military industries, thereby offering substantial economic and social benefits. In recent years, many studies have employed probabilistic methods to investigate the mechanical properties of materials [26-33], which can provide theoretical and technical support for further optimizing the design, manufacturing, and detection system performance of LVS in the future.

Acknowledgement

Thanks to Jiangsu Yindelong Wood Industry Co., Ltd. for their support of this study, including but not limited to site support and the provision of raw materials. Thanks to Professor Wang and Professor Mahmud Ashraf for his guidance and revisions of this article.

Funding Statement

The 2024 Forestry Science and Technology Innovation and Extension Project in Jiangsu Province (LYKJ[2024]05).

CRediT authorship contribution statement

Shuheng Yang: Writing-original draft, Writing review & editing, Visualization. **Zheng Wang**: Supervision, Resources, Writing-review & editing. **Mahmud Ashraf**: Writing - Review & Editing. **Zhaoyu Shen**: Conducting experiments, guiding the writing, visualization. **Yingchao Li**: experimental materials, testing facilities.

Conflicts of Interest

The authors declare that they have no conflicts of interest to report regarding the present study.

Data Availability Statement

Some or all data, models, or codes that support the findings of this study are available from the corresponding author upon reasonable request.

References

[1] Xie WB. Application Research of Laminated Veneer Lumber Dynamic Online Detection and Quality Classification. 2020, 10.27242/d.cnki.gnjlu.2020.000243.

[2] Yu XF. Manufactureing Process and Performance Analysis of Bamboo Laminated Veneer Lumber. 2012.

[3] ALBREKTAS D, IVANAUSKAS E. An Assessment of Environmental Impact on Glued Wood Building Elements. DRVNA INDUSTRIJA 2021, 72(1): 39-47. https://doi.org/10.5552/drvind.2021.2001.

[4] Li LZ, Yang L. Research on Fastgrowing Inorganic Composite Wood: Status and Prospect. World Forestry Research 2021, 34(05): 71-5. https://doi.org/10.13348/j.cnki.sjlyyj.2021.0054.y.

[5] Yao S, Pu JW. A comparative study on the physical and mechanical properties among three species of fast-growing poplar. Journal of Fujian Forestry Science and Technology 2008, (03): 148-52. https://doi.org/10.13428/j.cnki.fjlk.2008.03.038.

[6] Li WL, Xu W, Zhou XY, et al. Influence of cross lay-up structures on elastic constants and mechanical properties of poplar veneer laminated wood. Journal of Central South University of Forestry & Technology 2019, 39(05): 132-7. https://doi.org/10.14067/j.cnki.1673-923x.2019.05.019.

[7] Zuo KH, Xu WB, Li XY, et al. Research Status and Development of Laminated Veneer Lumber and Its Digital Simulation. China Forest Products Industry 2021, 58(01): 15-9. https://doi.org/10.19531/j.issn1001-5299.202101004.
[8] GILBERT B P, BAILLERES H, ZHANG H, et al. Strength modelling of Laminated Veneer Lumber (LVL) beams [J]. Construction and Building Materials, 2017, 149: 763-77. https://doi.org/https://doi.org/10.1016/j.conbuildmat.2017.05.153.
[9] MUSSELMAN E S, DINEHART D W, WALKER S M, et al. The effect of holes on the creep behavior and flexural capacity of laminated veneer lumber (LVL) beams [J]. CONSTRUCTION AND BUILDING MATERIALS, 2018, 180: 167-76. https://doi.org/10.1016/j.conbuildmat.2018.05.186.
[10] ZHOU H Y, WEI X, SMITH L M, et al. Evaluation of Uniformity of Bamboo Bundle Veneer and Bamboo Bundle Laminated Veneer Lumber (BLVL). FORESTS, 2019, 10(10). https://doi.org/10.3390/f10100921.
[11] Chang SY, Xing D, Wang XM, et al. Research Progress on Productive Technology and Properties of Laminated Veneer Lumber. China Forest Products Industry 2020, 57(07): 9-11+38. https://doi.org/10.19531/j.issn1001-5299.202007003.
[12] Hu YC, Gu JY, Wang FH. Developments and Prospects in the Research on NondestructiveTesting of Physical and Mechanical Properties of Wood and Wood Composites. World Forestry Research 2002, (04): 39-46. https://doi.org/10.13348/j.cnki.sjlyyj.2002.04.007.
[13] ZHANG L, HU Y C. Relationships between Dynamic Young's Modulus and Static MOE of the Reinforced Poplar LVL. MATERIALS AND MANUFACTURING TECHNOLOGY, PTS 1 AND 2. 2010: 588-91.10.4028/www.scientific.net/AMR.129-131.588
[14] Li WL, Xu W, Zhou XY, et al. Influence of cross lay-up structures on elastic constants and mechanical properties of poplar veneer laminated wood. Journal of Central South University of Forestry & Technology 2019, 39(05): 132-7. https://doi.org/10.14067/j.cnki.1673-923x.2019.05.019.
[15] DURIOT R, RESCALVO F J, POT G, et al. An insight into mechanical properties of heartwood and sapwood of large French Douglas-fir LVL [J]. CONSTRUCTION AND BUILDING MATERIALS, 2021, 299. https://doi.org/10.1016/j.conbuildmat.2021.123859.
[16] Yoshihara H, Kubojima Y. Measurement of the shear modulus of wood by asymmetric four-point bending tests[J]. Journal of Wood Science, 2002, 48(01):14-19. https://doi.org/10.1007/BF00766232
[17] Wang Z, Ghanem R. An extended polynomial chaos expansion for PDF characterization and variation with aleatory and epistemic uncertainties. Computer Methods in Applied Mechanics and Engineering 2021; 382, 113854. https://doi.org/10.1016/j.cma.2021.113854.
[18] Wang Z, Ghanem R. A functional global sensitivity measure and efficient reliability sensitivity analysis with respect to statistical parameters. Computer Methods in Applied Mechanics and Engineering 2022; 402, 115175. https://doi.org/10.1016/j.cma.2022.115175.
[19] Wang Z, Ghanem R. Stochastic framework for optimal control of planetary reentry trajectories under multilevel uncertainties. AIAA Journal 2023; 61(8), 257-3268. https://doi.org/10.2514/1.J062515.
[20] Wang Z, Hawi P, Masri S, Aitharaju V, Ghanem R. Stochastic multiscale modeling for quantifying statistical and model errors with application to composite materials. Reliability Engineering and System Safety 2023; 235, 109213. https://doi.org/10.1016/j.ress.2023.109213.
[21] Wang ZH, Ghanem R. Stochastic modeling and statistical calibration with model error and scarce data. Computer Methods in Applied Mechanics and Engineering 2023; 416, 116339. https://doi.org/10.1016/j.cma.2023.116339.
[22] Wang ZH, Gao ZZ, Wang YL, Cao Y, Wang GG, Liu B, Wang, Z. A new dynamic testing method for elastic, shear modulus and Poisson's ratio of concrete. Construction and Building Materials 2015; 100, 129-135. https://doi.org/10.1016/j.conbuildmat.2015.09.060.
[23] Yu TH, Wang ZH. Model updating of nonproportionally damped structural systems using an adapted complex sum-of-squares optimization algorithm. Journal of Engineering Mechanics 2023; 149(8), 04023043. https://doi.org/10.1061/JENMDT.EMENG-6953.
[24] Yu TH, Wang ZH, Wang JF. An iterative augmented unscented kalman filter for simultaneous state-parameter-input estimation for systems with/without direct feedthrough. Mechanical Systems and Signal Processing 2023; 205, 110793. https://doi.org/10.1016/j.ymssp.2023.110793.